ADVANCES IN ATMOSPHERIC SCIENCES, VOL. 30, NO. 3, 2013, 841–854

Steric Sea Level Change in Twentieth Century Historical Climate Simulation and IPCC-RCP8.5 Scenario Projection: A Comparison of Two Versions of FGOALS Model

DONG Lu[1,2] (董 璐) and ZHOU Tianjun*[1,3] (周天军)

[1] *State Key Laboratory of Numerical Modeling for Atmospheric Sciences and Geophysical Fluid Dynamics, Institute of Atmospheric Physics, Chinese Academy of Sciences, Beijing* 100029

[2] *University of the Chinese Academy of Sciences, Beijing* 100049

[3] *Climate Change Research Center, Chinese Academy of Sciences, Beijing* 100029

(Received 30 July 2012; revised 23 October 2012)

ABSTRACT

To reveal the steric sea level change in 20th century historical climate simulations and future climate change projections under the IPCC's Representative Concentration Pathway 8.5 (RCP8.5) scenario, the results of two versions of LASG/IAP's Flexible Global Ocean-Atmosphere-Land System model (FGOALS) are analyzed. Both models reasonably reproduce the mean dynamic sea level features, with a spatial pattern correlation coefficient of 0.97 with the observation. Characteristics of steric sea level changes in the 20th century historical climate simulations and RCP8.5 scenario projections are investigated. The results show that, in the 20th century, negative trends covered most parts of the global ocean. Under the RCP8.5 scenario, global-averaged steric sea level exhibits a pronounced rising trend throughout the 21st century and the general rising trend appears in most parts of the global ocean. The magnitude of the changes in the 21st century is much larger than that in the 20th century. By the year 2100, the global-averaged steric sea level anomaly is 18 cm and 10 cm relative to the year 1850 in the second spectral version of FGOALS (FGOALS-s2) and the second grid-point version of FGOALS (FGOALS-g2), respectively. The separate contribution of the thermosteric and halosteric components from various ocean layers is further evaluated. In the 20th century, the steric sea level changes in FGOALS-s2 (FGOALS-g2) are largely attributed to the thermosteric (halosteric) component relative to the pre-industrial control run. In contrast, in the 21st century, the thermosteric component, mainly from the upper 1000 m, dominates the steric sea level change in both models under the RCP8.5 scenario. In addition, the steric sea level change in the marginal sea of China is attributed to the thermosteric component.

Key words: steric sea level, historical climate simulation, RCP8.5 scenario, FGOALS model

Citation: Dong, L., and T. J. Zhou, 2013: Steric sea level change in twentieth century historical climate simulation and IPCC-RCP8.5 scenario projection: A comparison of two versions of the FGOALS model. *Adv. Atmos. Sci.*, **30**(3), 841–854, doi: 10.1007/s00376-012-2224-3.

1. Introduction

Sea level change is closely related to climate change and very important to the development of coastal regions and islands. Sea level rise in the world's oceans has been explored through the use of many datasets. Gornitz et al. (1982) and Gornitz and Lebedeff (1987) concluded that the rising rate of the global-averaged sea surface height (SSH) is about 12 cm per century based on tide gauge data. The result is based on 193 stations, with the records longer than 20 years prior to the year 1982 (Gornitz et al., 1982). Fairbridge and Krebs (1962) concluded a rising rate of 1.2 mm yr^{-1} for the period 1900–50 from selected stations. Klige (1982) showed a rising rate of 1.5 mm yr^{-1} for 1900–75. Barnett (1988) came to a result of 1.15 mm

*Corresponding author: ZHOU Tianjun, zhoutj@lasg.iap.ac.cn

yr^{-1} for 1880–1986 based on 155 stations. Satellite measurements show that SSH was rising at a rate of 3.4 mm yr^{-1} during the period 1993–2008 (Cazenave et al., 2009). This is almost twice the rising rate of the 20th century, which is about 1.7 mm yr^{-1} from tide gauge records (IPCC, 2007). Coastal tide gauge records indicate that similar rising rates have appeared in some earlier decades (IPCC, 2007). Based on the projection of sea level change from the 4th assessment report (AR4) of IPCC, the global-averaged SSH will rise by 0.22–0.44 m by the mid-2090s relative to the year 1990. Therefore, results can be inconsistent due to different datasets and time periods. Since SSH can directly reflect the strength of ocean gyres and 3D, large-scale ocean circulation, it is possible to use sea level changes to estimate the Atlantic Meridional Overturning Circulation (Häkkinen, 2001; Landerer et al., 2007). Therefore, identifying the features of sea level changes and predicting/projecting near-future (refer here to the IPCC's Representative Concentration Pathway 8.5 (RCP8.5) projection: 2006–2100) SSH changes are of crucial importance to climate change research and ocean circulation studies.

Global sea level changes through a diverse range of processes, such as a change in absolute ocean mass, variation in ocean salinity, and a change of specific volume through net heating or cooling (Landerer et al., 2007). The expansion or contraction of the oceans through density change is a single component of entire sea level change, commonly called "steric sea level change". The term "steric" is used here as pertaining to the volume of the ocean depending on temperature, salinity and pressure (Landerer et al., 2007). The mechanisms responsible for global and regional sea level changes have been discussed in many modeling studies (e.g. Mikolajewicz et al., 1990; Bryan, 1996; Knutti and Stocker, 2000; Mikolajewicz and Voss, 2000; Gregory et al., 2001; Levermann et al., 2005). However, the projected spatial patterns and causes of sea level changes remain different from one model to another (Gregory et al., 2001; Landerer et al., 2007). Much more effort has been devoted to the assessment of various factors contributing to sea level rise since the IPCC's AR4 report, with the study of global sea level rise receiving considerable attention in recent decades (e.g. Gregory et al., 2001; Antonov et al., 2002; Munk, 2002; Cazenave and Nerem, 2004; Antonov et al., 2005).

Boussinesq approximation (Boussinesq, 1903) is a classical assumption in ocean models. In this assumption, conservation of volume is applied instead of mass conservation. However, the volume response of the global ocean to global warming is not conservative. In recent decades, global-averaged sea level has risen mainly due to thermal expansion of seawater under global warming (Church et al., 1991; Wu et al., 2006). Under the IPCC's Special Report on Emission Scenarios (SRES) A1B scenario, more than half of the projected global sea level rise is attributed to thermal expansion (IPCC, 2007). The Boussinesq approximation models based on volume conservation cannot reproduce such kinds of physical processes and thus are unable to correctly capture the global steric sea level rise related to ocean density changes (Greatbatch, 1994). Instead, we need to recalculate steric sea level through ocean density models of this kind.

Two versions of the State Key Laboratory of Numerical Modeling for Atmospheric Sciences and Geophysical Fluid Dynamics, Institute of Atmospheric Physics (LASG/IAP's) coupled climate system model Flexible Global Ocean-Atmosphere-Land System (FGOALS) have been participating in the ongoing Coupled Model Intercomparison Project Phase 5 (CMIP5) experiments (http://pcmdi3.llnl.gov/esgcet/home.htm) for the IPCC's AR5 report. However, the performance of FGOALS in sea level change simulation and projection has never been examined. Accordingly, this paper aims to answer the following questions: (1) How well do the two versions of FGOALS simulate the global SSH pattern? (2) What were the characteristics of steric sea level change in the 20th century according to historical climate simulations performed by the two versions of FGOALS? (3) How will global steric sea level change in the 21st century under the IPCC's AR5 RCP8.5 scenario projection? (4) Are there any differences between the two versions of FGOALS in projecting future global and regional sea level changes? In this work, we focus on the steric sea level change due to density changes of the ocean in the 20th century historical climate simulations and the 21st century projections under the RCP8.5 scenario. We show evidence that global-averaged steric sea level will have a pronounced rising trend throughout the 21st century under the RCP8.5 scenario. The magnitude of steric sea level change in the 21st century is much larger than that in the 20th century. In the historical climate simulations, steric sea level changes are largely attributed to the thermosteric component in the second spectral version of FGOALS (FGOALS-s2), while in the second grid-point version of FGOALS (FGOALS-g2) they are mainly attributed to the halosteric component. In contrast, the contributions of the thermosteric component dominate the steric sea level change under the RCP8.5 scenario projections in both models.

The remainder of the paper is organized as follows. Section 2 introduces the models, experiments and analysis methods. The global and regional steric sea

level changes and the individual contributions of the thermosteric and halosteric components in the 20th century historical climate simulations and RCP8.5 scenario projections are analyzed in section 3. Finally, a summary is presented in section 4.

2. Model and method description

2.1 *Model, experiments, and data description*

The CMIP5 experiments of the two versions of the LASG/IAP's coupled climate system model FGOALS are analyzed. The first is the second spectral version of FGOALS, known as FGOALS-s2 (Bao et al., 2013), and the second is the grid-point Version 2, known as FGOALS-g2 (Li et al., 2013). These two versions of FGOALS are identical in their ocean, land, and coupler components, but employ different AGCM (atmosphere general circulation model) and sea ice components. The ocean component of FGOALS is the LASG/IAP's Climate System Ocean Model version 2 (LICOM2), which has a horizontal resolution of about $1^\circ\times1^\circ$ in the extra-tropical zone and $0.5^\circ\times0.5^\circ$ in the tropics, and 30 vertical levels. The land component is the Community Land Model version 3 (CLM3). For FGOALS-s2, the atmospheric component is the Spectral Atmospheric Model of the IAP/LASG's version 2 (SAMIL2), with a horizontal resolution of about 2.81° (lon)$\times1.66^\circ$ (lat) and 26 levels in the vertical direction. For FGOALS-g2, the atmospheric component is the Grid-point Atmospheric Model of the IAP/LASG, Version 2 (GAMIL2), with a horizontal resolution of about $2.8^\circ\times2.8^\circ$ and 26 levels in the vertical direction. The sea ice component of FGOALS-s2 is the Community Sea Ice Model version 5 (CSIM5), while in FGOALS-g2 it is the Los Alamos Sea Ice Model (CICE). All four components are coupled together by the NCAR's flux coupler module, version 6 (CPL6). For more details of the various model components, readers are referred to Bao et al. (2013) and Li et al. (2013).

The outputs of three sets of model experiments are used in this study: (1) 20th century historical climate simulations (1850–2005); (2) future climate change projections under the RCP8.5 scenario (2006–2100); and (3) a 500-yr pre-industrial control run. For details of these experiments, please see Taylor et al. (2012). In the analysis, we convert the monthly products of these experiments to yearly variables.

In addition to model data, objective analysis dynamic ocean topography data was also used (Maximenko et al., 2009). This dataset is constructed using satellite altimetry, near-surface drifters, National Centers for Environmental Prediction (NCEP) wind, and the geoid model of the Gravity Recovery and Climate Experiment (GRACE). The data represents mean dynamic ocean topography, averaged for 1993–2002, and is available at a spatial resolution of $0.5^\circ\times0.5^\circ$ (http://apdrc.soest.hawaii.edu/projects/DOT).

2.2 *Analysis method*

The oceanic component of FGOALS is LICOM, which applies the Boussinesq approximation (Liu et al., 2004). The SSH predicted by the model is based on the conservation of volume, which is called "dynamic sea level". The term "dynamic" represents the geostrophic balance between horizontal flow and SSH gradients, so the flow is along the contours of equal SSH (Gill, 1982). As stated in the Introduction part, the dynamic sea level predicted by LICOM cannot capture the sea level changes associated with expansion or contraction of the oceans due to density change. Therefore, to examine the predicted sea level change due to global warming, we need to recalculate steric sea level by ocean density from LICOM. As shown below, the calculation is based on mass conservation (Li et al., 2003).

The mass conservation equation is written as:

$$\frac{\partial\rho}{\partial t}+\frac{\partial(\rho u)}{\partial x}+\frac{\partial(\rho v)}{\partial y}+\frac{\partial(\rho w)}{\partial z}=0\,, \tag{1}$$

where ρ is density of seawater and u, v, w denote 3D ocean current velocity. Based on this relationship, we obtain the steric SSH ($H_{\rm s}$) tendency equation (Li et al., 2003):

$$\frac{\partial H_{\rm s}}{\partial t}=-\frac{1}{\rho_0}\int_H^0\frac{\partial\rho}{\partial t}dz\,, \tag{2}$$

where $H_{\rm s}$ is the SSH caused by local density changes due to vertical expansion or contraction of the ocean column and H represents the sea bottom depth. It is the main component of local sea level changes from seasonal to climate change time scales (Church et al., 1991; Pattullo et al., 1955). Here, ρ_0 is 1026 kg m^{-3}.

Based on Eq. (2), the steric SSH changes relative to the year 1850 are calculated as follows:

$$H_{{\rm s},t}=\int_H^0\frac{\rho_{1850}-\rho_t}{\rho_0}dz\,. \tag{3}$$

Following Landerer et al. (2007), the changes of entire steric SSH are further decomposed into two parts: the thermosteric component and halosteric component. The individual contribution to the entire steric SSH change relative to the control run is calculated as:

$$H_{\rm s,thermo}=\int_{-H}^0\frac{\rho(S_{\rm C},T_{\rm C},p)-\rho(S_{\rm C},T_{\rm EX},p)}{\rho(S_{\rm C},T_{\rm C},p)}dz\,, \tag{4}$$

$$H_{\rm s,halo}=\int_{-H}^0\frac{\rho(S_{\rm C},T_{\rm C},p)-\rho(S_{\rm EX},T_{\rm C},p)}{\rho(S_{\rm C},T_{\rm C},p)}dz\,, \tag{5}$$

where the subscript EX refers to the 20th century historical climate simulations or RCP8.5 scenario projections, C refers to the control run fields, and ρ represents the in situ density, depending on salinity S, temperature T and pressure p (Gill, 1982).

Based on Eqs. (4) and (5), we can estimate the individual effect of temperature and salinity on the entire steric SSH changes relative to the fields of the control run. It is demonstrated that the sum of the two individual effects can reasonably reproduce the entire steric SSH field, with the difference between them at least two orders of magnitude smaller than the entire steric signals (Landerer et al., 2007).

3. Results

In the following analysis, we firstly examine the mean dynamic sea level (commonly called "dynamic ocean topography") in the two versions of FGOALS by comparing the model results to an objective analysis dataset. Then, we evaluate the steric sea level changes and separate contributions of the thermosteric and halosteric components in the 20th century historical climate simulations. Finally, we analyze the steric sea level changes in the future climate change projections under the RCP8.5 scenario and discuss the differences between FGOALS-s2 and FGOALS-g2.

3.1 *Mean dynamic sea level*

The dynamic sea level is closely linked to ocean currents through geostrophic balance, which indicates the deviation of SSH from the global mean (Yin et al., 2010). To examine the performance of the FGOALS models in simulating sea level distribution, we firstly assess the simulated mean dynamic sea level by comparing model results to an objective analysis dataset (Maximenko et al., 2009). Because the steric sea level is calculated from Eq. (3), we can only obtain a SSH anomaly pattern relative to the year 1850. We use the dynamic sea level to assess the performance of the models in simulating sea level distribution because the objective analysis dataset provides dynamic sea level data. In addition, though their physical processes are quite different, the dynamic sea level and steric sea level have similar patterns based on model results, especially in the tropics (Li et al., 2003).

The control runs of the two versions of FGOALS reasonably reproduced the distribution of mean dynamic sea level, which reflects ocean topography features (Fig. 1). The spatial pattern correlation coefficient between the simulation and the observation is 0.97 for both FGOALS-s2 and FGOALS-g2. The corresponding RMSE is 0.177 m (0.172 m) for FGOALS-s2 (FGOALS-g2). In the western boundary currents regions, such as the Gulf Stream and Kuroshio, the dynamic sea level gradients are evidently sharp. The highest (lowest) dynamic sea level value is found in the western North Pacific (the Southern Ocean). The strongest gradient also occurs in the Southern Ocean, which is associated with the Antarctic Circumpolar Current (ACC). The comparison to the observation indicates a reasonable performance of the two versions of FGOALS.

In the following analysis, we focus on the steric sea level change, because in both the 20th century historical climate simulations and future climate change projections, the sea level changes caused by the expansion or contraction of the ocean volume under global warming play important roles.

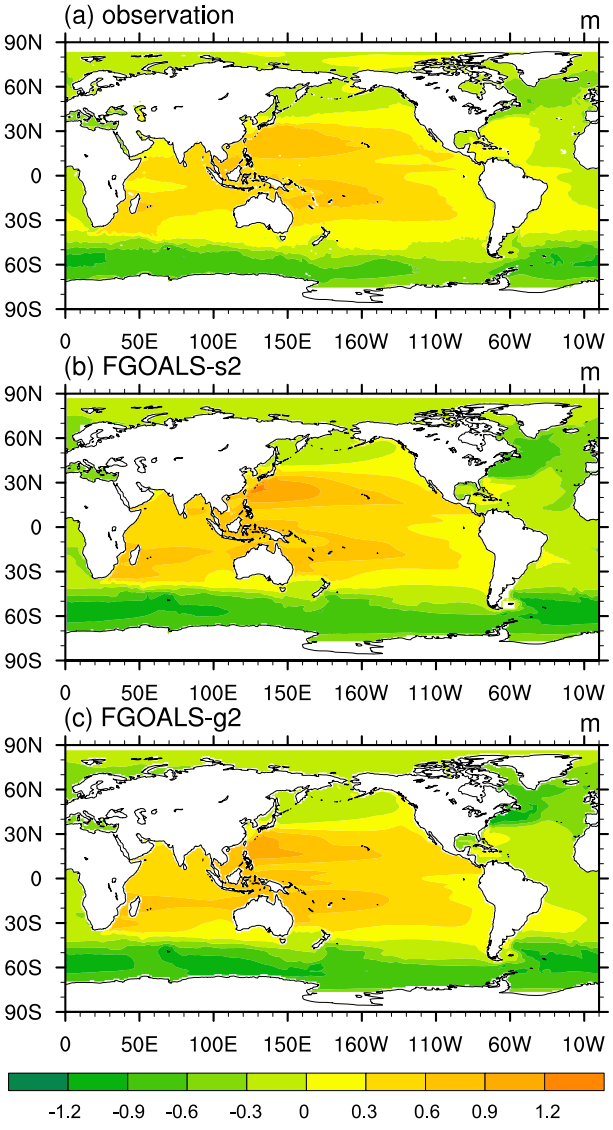

Fig. 1. Mean dynamic ocean topography from (a) observation, (b) FGOALS-s2, (c) FGOALS-g2. Units: m.

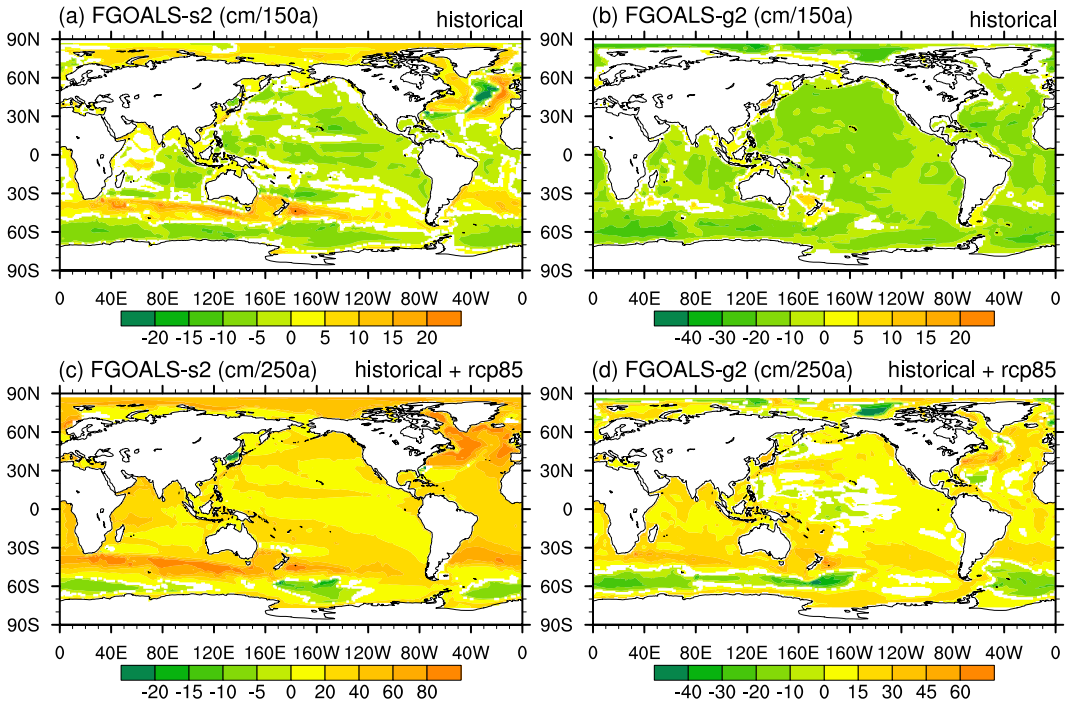

Fig. 2. Linear trends of SSH in (a, b) historical simulations (1850–2005) and (c, d) historical and RCP8.5 simulations (1850–2100) with FGOALS-s2 and FGOALS-g2. The shaded areas are statistically significant at the 5% level.

3.2 *Steric sea level change in the 20th century historical climate simulations*

We firstly examine the spatial pattern of the steric sea level trends in the 20th century historical climate simulations (1850–2005). The negative trends cover most parts of the global ocean in both models (Figs. 2a and b). The trends are not the same in different oceans in FGOALS-s2, with a rising trend mainly appearing in the Arctic Ocean and mid-latitude oceans in the Southern Hemisphere (Fig. 2a). In particular, the steric sea level in the marginal sea of China is rising in FGOALS-s2, but the trend is not significant in FGOALS-g2.

The temporal evolution of global annual mean and basin-averaged relative steric sea level height anomalies during 1850–2005 are shown in Fig. 3. There is no significant trend in global-averaged sea level evolution in the historical climate simulation of FGOALS-s2, while FGOALS-g2 shows a weak falling trend during the period 1850–2005. The trends are -0.03 mm yr^{-1} and -0.3 mm yr^{-1} for FGOALS-s2 and FGOALS-g2, respectively (Figs. 3a and b). The SSH anomalies in different oceans are of different orders of magnitude. The results from satellite data and hydrographic observations show a uniformly rising pattern around the world's oceans, which confirms the results of climate models (IPCC, 2007). In both models, the change of the Arctic Ocean is higher than the global average, while the changes of other oceans are consistent with the global average, with relative SSH anomalies close to zero (Figs. 3c–f).

To distinguish the contributions of temperature and salinity to the entire steric sea level change in the 20th century historical climate simulations, we estimate the thermosteric and halosteric effects relative to the control run. For the average of the period 1990–99, the steric sea level changes relative to the control run are positive for most parts of the global ocean, and the magnitude in FGOALS-g2 is larger than that in FGOALS-s2 (Figs. 4a and b). The steric sea level changes are largely attributed to the thermosteric (halosteric) component in FGOALS-s2 (FGOALS-g2). For the global average of steric sea level change, the contribution of the thermosteric component accounts for about 106.7% and 31.6% for FGOALS-s2 and FGOALS-g2, respectively. The weak contribution in FGOALS-g2 may result from the treatment of water flux exchanges in the model, since runoff from land sources does not discharge into the ocean in this model and thus the water process is not balanced. This partly explains why the ocean salinity has a stronger and unconscionable change in FGOALS-g2 in comparison to FGOALS-s2. Antonov et al. (2002) suggest that only about 10% of the global-averaged steric sea level rise can be attributed to the halosteric component in re-

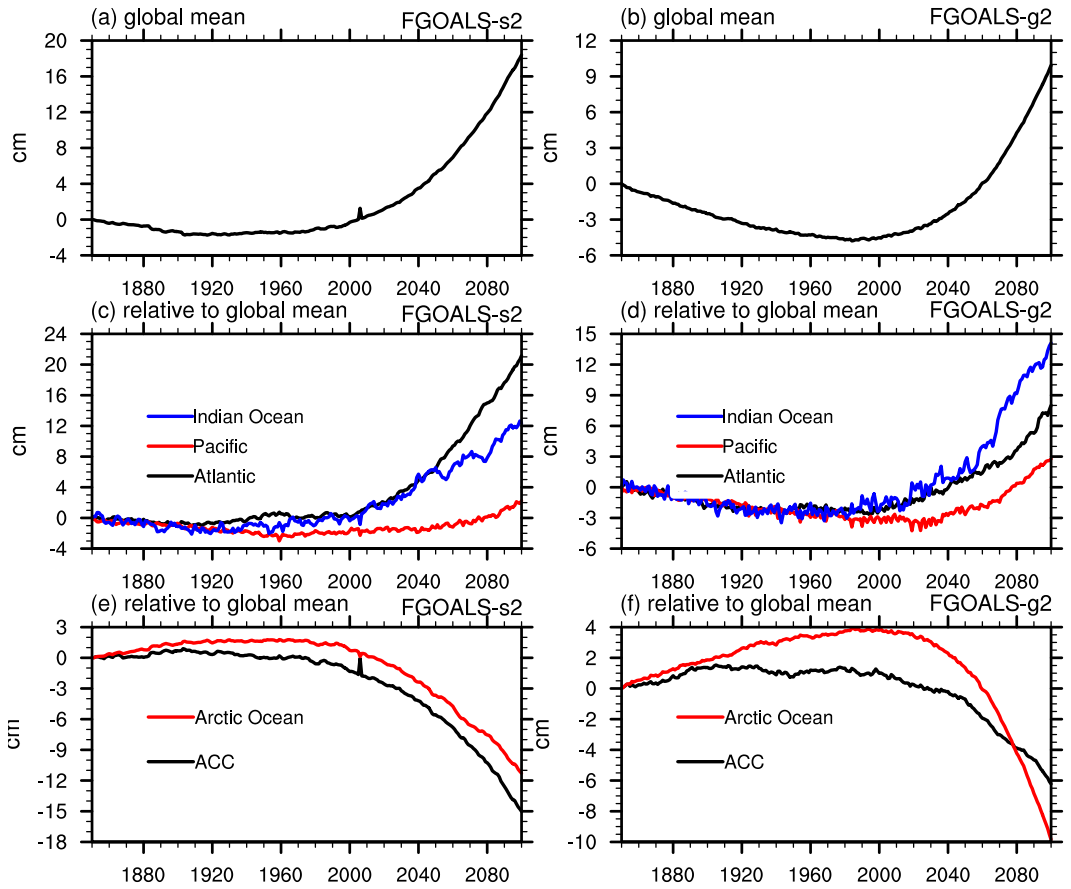

Fig. 3. Time series of global annual mean SSH anomaly from (a) FGOALS-s2 and (b) FGOALS-g2. Basin-averaged evolution of SSH anomalies: deviation from the global mean change in (a, b) at corresponding times: (c, d) Indian Ocean (40°S–15°N, 45°–105°E), Pacific (30°–65°N, 120°E–105°W), and Atlantic (40°S–65°N, 50°W–0°) SSH and (e, f) ACC (80°–55°S, 180°W–180°E) and Arctic Ocean (75°–90°N, 180°W–180°E) SSH. Units: cm.

cent decades. However, it is revealed in IPCC AR4 that, for the regional scale, the contributions of the thermosteric and halosteric components can be comparably important. As a result, although ocean salinity is not important for steric sea level changes at the global scale, it plays a role at the regional scale (e.g. Antonov et al., 2002; Ishii et al., 2006).

Similar to the changes in most parts of the global ocean, the steric sea level in the marginal sea of China shows a positive change relative to the control run in both models, but with a weak negative change in part of the East China Sea in FGOALS-g2 (Figs. 4a and b). In both models, the thermosteric component makes positive contributions to the steric sea level change in the marginal sea of China (Figs. 4c and d), while the halosteric component makes negative contributions (Figs. 4e and f).

Because steric sea level is the result of vertical integration throughout the whole depth, we further investigate the vertical structure of the steric sea level changes relative to the control run for the average of the period 1990–99. The contributions of the thermosteric and halosteric components from each layer were cumulatively summed up from the sea surface to the deepest layer in the model, and the results are shown in Figs. 5 and 6. In FGOALS-s2, for the global average the thermosteric component is larger than the halosteric component throughout the depth, with the largest contribution from the upper 1000 m (Fig. 5a). At the basin scale, the vertical structure in the Pacific, Atlantic and Indian Oceans are similar to the global average. In the ACC, the effects from the thermosteric and halosteric components are evident in the upper 3000 m. For the Arctic Ocean, the halosteric component dominates the entire steric sea level changes in the upper 1000 m. In contrast, in FGOALS-g2 the halosteric component is larger than the thermosteric component throughout the whole depth for the global average (Fig. 6a). The result is consistent with that in Fig. 4. The vertical structure in the Pacific Ocean,

Fig. 4. (a, b) Steric SSH difference for the average of the period 1990–99 relative to the control run. (c, d) Thermosteric component as defined in Eq. (4). (e, f) Halosteric component as defined in Eq. (5). Units: cm.

Indian Ocean and the ACC are similar to the global average. For the Atlantic, the contributions of the two components are comparable in the upper 2000 m, but below 2000 m the thermosteric component dominates the entire steric sea level change. For the Arctic Ocean, the contributions of the two components compensate each other, but the thermosteric component has a larger negative value.

3.3 *Future steric sea level change under the IPCC's RCP*8.5 *scenario*

In this section, we focus on the future steric sea level changes in the 21st century projections, under the RCP8.5 scenario, which is a response to global warming forced by increased greenhouse gas (GHG) concentrations. For the period 1850–2100, the steric sea level shows a general rising trend in most parts of the global ocean except for several areas of the Southern Ocean (Figs. 2c and d). In addition, the steric sea level in the marginal sea of China shows a rising trend in both models.

The global-averaged steric sea level evolution shows a pronounced rising trend throughout the 21st century under the RCP8.5 scenario in both models (Figs. 3a and b). A constant acceleration in global-averaged steric sea level rise during the 21st century has been evaluated by many coupled atmosphere-ocean general circulation models (Gregory et al., 2001). The pronounced increasing value is from the year 2006, when the RCP8.5 simulation begins. By the year 2100, the global warming under RCP8.5 scenario produces a steric SSH anomaly of 18 cm and 10 cm relative to the year 1850 in FGOALS-s2 and FGOALS-g2, respectively. In our study, as projected under the RCP8.5 scenario, the changes in different oceans in the 21st century are more inconsistent than those in the 20th

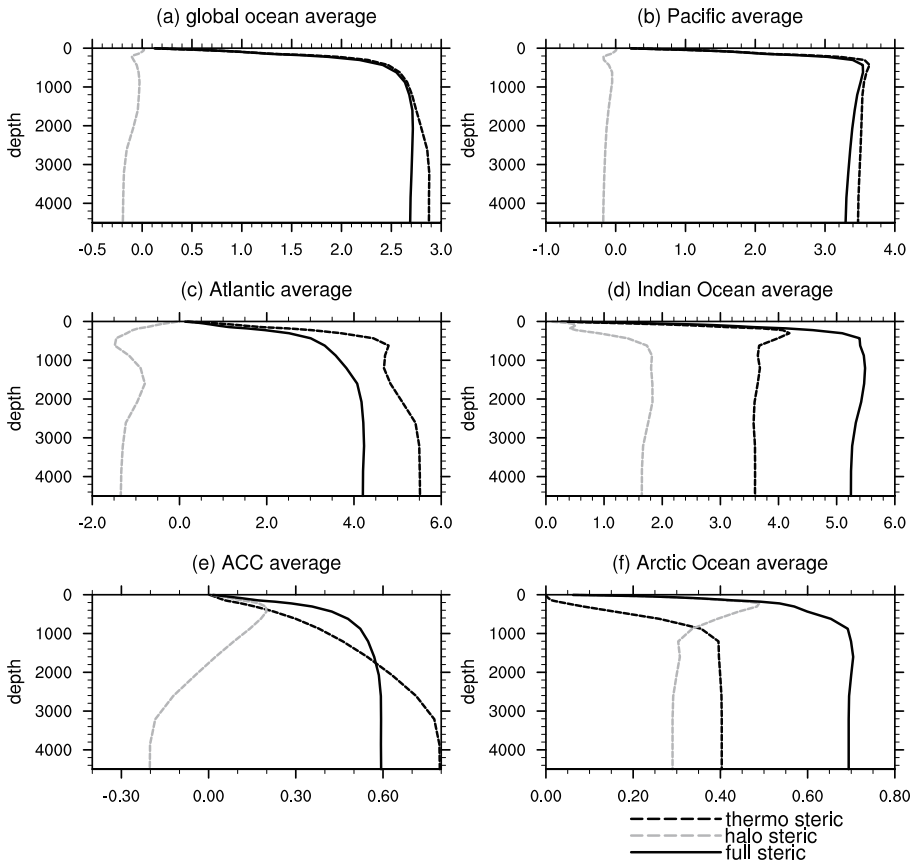

Fig. 5. Cumulative sum of thermosteric (black dashed line), halosteric (gray dashed line), and total steric SSH (black line) anomalies for different ocean areas from FGOALS-s2 for the average of the period 1990–99 relative to the control run. Starting at the surface, the steric SSH anomaly from each depth layer is added up. Units: cm.

century historical climate simulation. The steric sea level averaged in the Arctic Ocean and the ACC are much lower than that of the global average (Figs. 3e and f), but in the Atlantic and Indian Oceans are much higher than that of the global average. The change in the Pacific is nearly consistent with that of the global average (Figs. 3c and d). Note that this result is different from the basin-averaged evolution of dynamic SSH anomalies in the Max Planck Institute for Meteorology (MPI) coupled atmosphere-ocean general circulation model (ECHAM5/MPI-OM) under the IPCC's A1B climate change scenario (Landerer et al., 2007). In previous studies, nearly all models show that the dynamic sea level rise in the Arctic Ocean (Southern Ocean) is more (less) than that of the global average (Gregory et al., 2001). However, this feature is not evident in the results of the steric sea level from the two versions of FGOALS. This may be due to the differences between the two kinds of sea level, as well as model-dependence. Gregory et al. (2001) argued that the simulated regional sea level changes from various models are different from each other and lack agreement about the distribution of these regional patterns. As reported in IPCC AR4 (2007), the spatial variability of sea level change is mainly due to the non-uniform changes in temperature, salinity and associated ocean circulation. Therefore, the patterns of temperature, salinity and ocean circulation should be further examined.

The individual contribution of the thermosteric and halosteric components relative to the control run is further evaluated in the following. For the average of the period 2090–99, the steric sea level changes relative to the control run are positive in almost all the oceans, and with a much larger magnitude than those in the historical climate simulation (Figs. 7a and b). The separate evaluation of the thermosteric and halosteric components shows that the contribution of

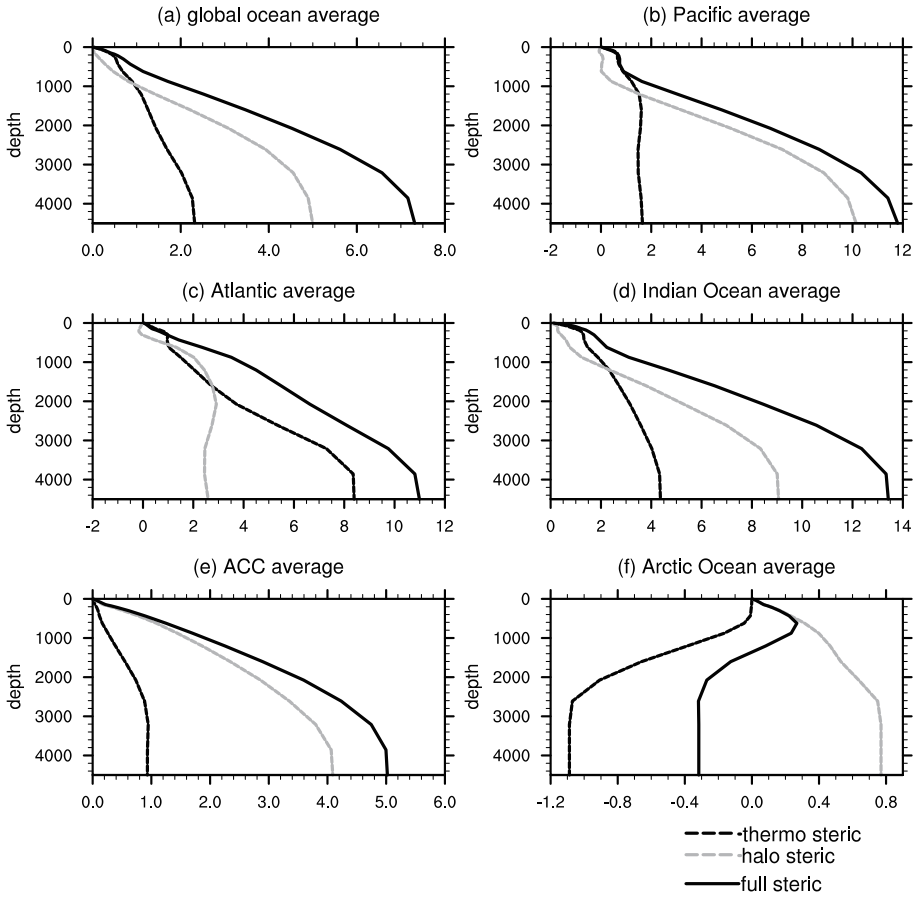

Fig. 6. The same as Fig. 5, but for FGOALS-g2. Units: cm.

the thermosteric component is positive over most parts of the global ocean (Figs. 7c and d). The most significant signal of the thermosteric component is in the Atlantic, while the Arctic and ACC show a weak signal. As Yin et al. (2010) has pointed out, in a warming climate projection the deeper oceans can absorb more heat and therefore show a stronger thermosteric signal. The signs of the halosteric component are different in different ocean basins (Figs. 7e and f). A similar result is seen in the ECHAM5/MPI-OM model result for the IPCC A1B scenario (Landerer et al., 2007). The steric sea level changes are largely attributed to the thermosteric component. For global-averaged change, the contribution of the thermosteric component accounts for about 105.7% and 81.8% for FGOALS-s2 and FGOALS-g2, respectively. Although FGOALS-g2 does not include runoff from land sources, under the RCP8.5 scenario the ocean temperature shows a significant warming trend that overwhelms the effect of ocean salinity changes. Therefore, it is the thermosteric component that dominates the steric sea level change in both models under RCP8.5 scenario projection. We find that the most pronounced signals appear in the subtropical North Atlantic, with positive anomalies for the thermosteric component and negative anomalies for the halosteric component. In addition, the steric sea level in the marginal sea of China shows a weak positive change relative to the control run (Figs. 7a and b). In both models, the thermosteric (halosteric) component has a positive (negative) contribution to the final changes of entire steric sea level in the marginal sea of China (Figs. 7c–f). This conclusion is similar to that from the 20th century historical climate simulation results.

The dominance of the thermosteric and halosteric components may be depth-dependent. To examine this hypothesis, the vertical structures of the two steric sea level components relative to the control run under RCP8.5 scenario projection are shown in Figs. 8 and 9. Generally, the thermosteric component is much larger than the halosteric component in global-averaged contribution throughout the depth. The largest contributions are mainly due to the upper 1000 m in FGOALS-s2, while the contributions in FGOALS-g2 are slightly deeper, especially for the thermosteric component contribution (Figs. 8a and 9a). At the basin scale, the ver-

Fig. 7. The same as Fig. 4, but for the average of the period 2090–99.

tical structures in the Pacific and Atlantic are similar to the global average in both models. In the Indian Ocean, the thermosteric component prevails throughout the depth in FGOALS-s2, while the halosteric component prevails within the upper 1000 m and the two components are comparable below 1000 m in FGOALS-g2. The responses averaged in the ACC and the Arctic Ocean are much smaller than the other oceans in amplitude. In the ACC region, the contributions of the thermosteric and halosteric components in FGOALS-s2 are similar in the upper 500 m, but below 500 m the thermosteric component dominates the final change (Fig. 8e). In contrast, the halosteric component is slightly larger than the thermosteric component in the upper 1500 m, but slightly smaller than the thermosteric component below 1500 m in FGOALS-g2 (Fig. 9e). For the Arctic Ocean, the halosteric component dominates the steric sea level change in FGOALS-s2 (Fig. 8f). While the halosteric component is larger than the thermosteric component in the upper 1000 m, the two components tend to compensate each other, resulting in the entire steric sea level change being close to zero below 1000 m in FGOALS-g2 (Fig. 9f). In summary, halosteric sea level change is important in the Arctic Ocean. Our model results are consistent with many previous studies in this regard (Landerer et al., 2007; Yin et al., 2010).

4. Summary and discussion

4.1 *Summary*

To reveal the steric sea level change in the 20th century century historical climate simulation and future climate change projection under the RCP8.5 scenario, the results of two versions of the LASG/IAP's FGOALS model were analyzed. Characteristics of steric SSH changes in historical climate simulation and under RCP8.5 scenario projection were revealed. To distinguish the contributions of temperature and salinity to the entire steric sea level change, separate

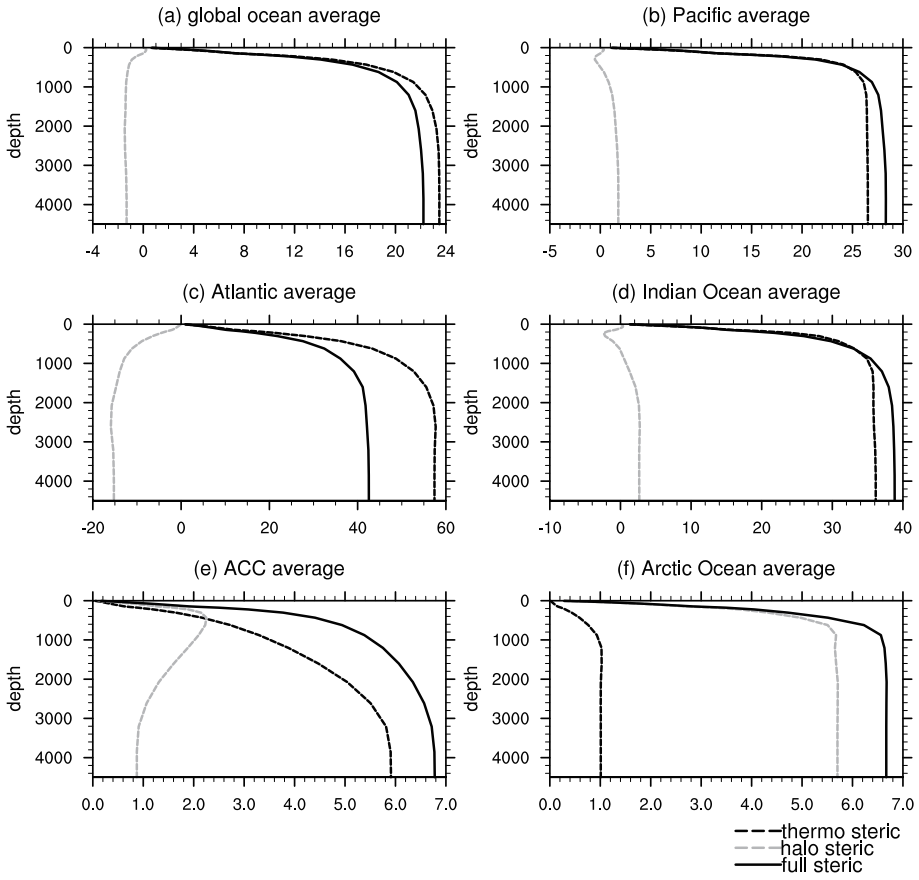

Fig. 8. Cumulative sum of thermosteric (black dashed line), halosteric (gray dashed line), and total steric SSH (black line) anomalies for different ocean areas from FGOALS-s2 for the average of the period 2090–99 relative to the control run. Starting at the surface, the steric anomaly from each depth layer is added up. Units: cm.

contributions of thermosteric and halosteric components were evaluated. The steric sea level changes relative to the control run in different oceans from various ocean layers were assessed. The main conclusions are as follows:

(1) Both versions of FGOALS reasonably reproduced the mean dynamic sea level features in comparison to an objective analysis dataset. The spatial pattern correlation coefficient between the simulation and the observation was 0.97 for both FGOALS-s2 and FGOALS-g2, and the corresponding RMSE was 0.177 m (0.172 m) for FGOALS-s2 (FGOALS-g2).

(2) In the 20th century historical climate simulations, negative trends covered most of the global ocean. The steric sea level changes could be largely attributed to the thermosteric contribution in FGOALS-s2, but to the halosteric contribution in FGOALS-g2. For global-averaged steric sea level change, the contribution of the thermosteric component accounted for about 106.7% and 31.6% for the average of the period 1990–99 relative to the control run in FGOALS-s2 and FGOALS-g2, respectively. The contributions were found to be mainly from the upper 1000 m in FGOALS-s2, but from the whole depth in FGOALS-g2.

(3) Under RCP8.5 scenario projection in both models, a pronounced rising trend in global-averaged steric sea level throughout the 21st century was found, and a general rising sea level trend appeared in most parts of the global ocean. The magnitude of steric sea level change in the 21st century was modeled to be much larger than that in the 20th century.

(4) There were some differences found between the two versions of FGOALS in projecting future steric sea level change. Specifically, by the year 2100, the steric SSH anomaly will be 18 cm and 10 cm relative to the year 1850 according to FGOALS-s2 and FGOALS-g2, respectively. The steric sea level changes were largely attributed to the thermosteric component, and mainly from the upper 1000 m in both models. For global-averaged change, the thermosteric component accounted for about 105.7% and 81.8% for the

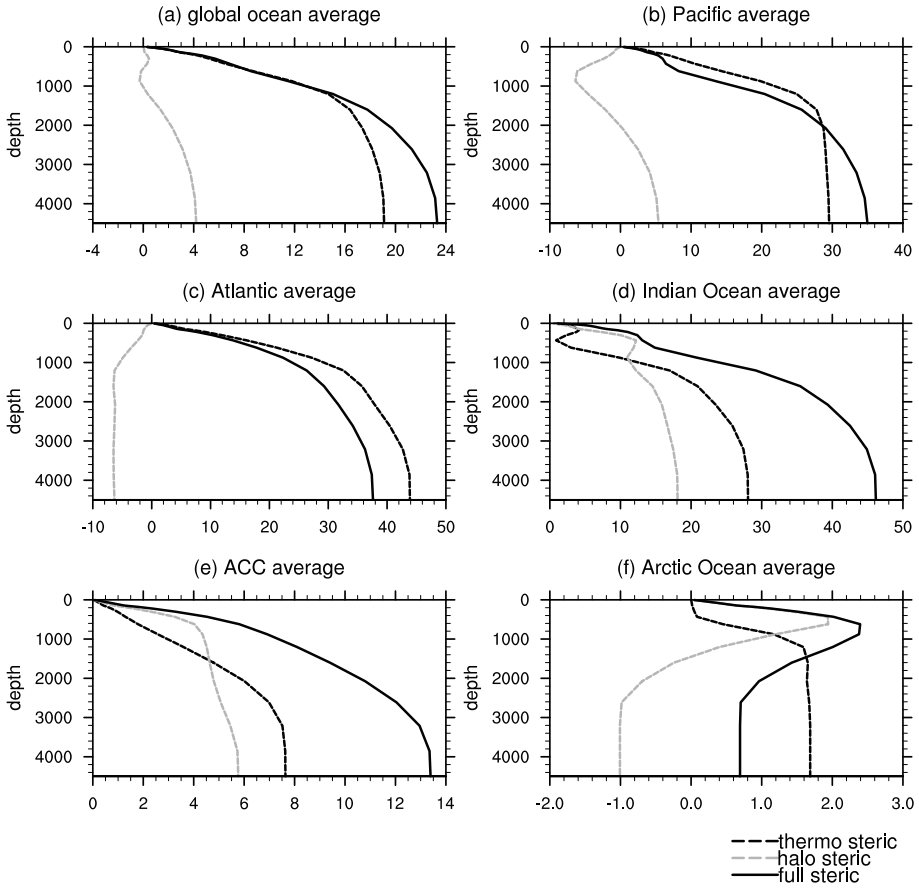

Fig. 9. The same as Fig. 8, but for FGOALS-g2. Units: cm.

average of the period 2090–99 relative to the control run in FGOALS-s2 and FGOALS-g2, respectively.

(5) The steric sea level in the marginal sea of China will rise in future climate change projection under the RCP8.5 scenario. In both 20th century climate simulation and 21st century projection under the RCP8.5 scenario, positive changes relative to the control run were found in the marginal sea of China. The positive changes were attributed to the thermosteric component.

4.2 *Discussion*

The limitations of the current study should be acknowledged. The performance of FGOALS in the projection of steric sea level change under the RCP8.5 scenario was firstly examined. While the main results were consistent with previous studies, e.g. the pronounced rising trend and the dominance of the thermosteric component in the entire steric sea level change in the 21st century, differences were seen in the steric sea level changes simulated by the two versions of FGOALS. The most significant difference was that, in the 20th century, the steric sea level changes were largely attributed to the thermosteric (halosteric) component in FGOALS-s2 (FGOALS-g2). The reason for the difference remains unknown. Further analysis on the water flux budget across the ocean–atmosphere and land–ocean boundaries is needed in future work.

The differences in the ocean mass structure and its

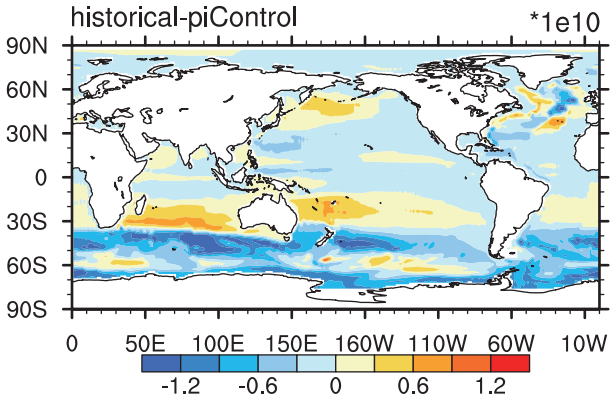

Fig. 10. The ocean barotropic mass stream function for the average of the period 1990–99 from the differences pattern between historical simulation and the pre-industrial control run. Units: Kg s^{-1}.

associated ocean circulation features may also lead to different results between models (Yin et al., 2010). Changes in ocean circulation are important to sea level changes, mainly at the decadal scale and local or regional scales (Bryan, 1996; Landerer et al., 2007). Large-scale ocean circulation changes may redistribute ocean water masses and, thus, lead to different steric sea level changes regionally (Landerer et al., 2007). To understand the effects of ocean circulation on the changes of sea level, we show the differences pattern in the ocean barotropic mass stream function between the 20th century historical climate simulation and pre-industrial control run from FGOALS-s2 in Fig. 10. The change of ocean circulation has a similar pattern to the steric sea level changes, especially in the North Atlantic and Southern Ocean (cf. Fig. 10 to Fig. 4a), demonstrating that the ocean circulation changes may impact the sea level changes patterns, especially at the regional scale.

Our estimation of the steric sea level change is based on mass conservation. While steric sea level change is a useful reference for total sea level changes, we note that in observations the contribution of steric sea level rise has decreased due to the increased melting of sea ice in recent years (Church et al., 2011), so sea level rise caused by mass change should also be studied in future work.

The CMIP5 has designed several scenarios for future climate change projection. This study focused on RCP8.5, which is a rather tough projection of future changes. In forthcoming work, we will examine the sea level changes under other scenarios, such as RCP4.5 and RCP6. By comparing them, we can investigate the response of SSH to different strengths of greenhouse gases increase at the global as well as regional scale.

Finally, we acknowledge that there are different points of view on the nature of sea level changes. For instance, Dobrovolski (2000) suggested that year-to-year global sea level changes during the 20th century are satisfactorily described by the discrete Wiener process model, which indicated that sea level change was a stochastic process. The nature of sea level changes also deserves further study.

Acknowledgements. This work was jointly supported by the National High Technology Research and Development Program of China (863 Program) under Grant No. 2010AA012304, the "Strategic Priority Research Program–Climate Change: Carbon Budget and Related Issues" of the Chinese Academy of Sciences (Grant No. XDA05110301), and the National Natural Science Foundation of China (Grant Nos. 41125017 and 40890054).

REFERENCES

Antonov, J. I., S. Levitus, and T. P. Boyer, 2002: Steric sea level variations during 1957–1994: Importance of salinity. *J. Geophys. Res.*, **107**, 8031, doi: 10.1029/2001JC000964.

Antonov, J. I., S. Levitus, and T. P. Boyer, 2005: Thermosteric sea level rise, 1955–2003. *Geophys. Res. Lett.,* **32**, L12602, doi: 10.1029/2005GL023112.

Bao, Q., and Coauthors, 2013: The Flexible Global Ocean-Atmosphere-Land System model Version 2: FGOALS-s2. *Adv. Atmos. Sci.*, doi: 10.1007/s00376-012-2113-9.

Barnett, T. P., 1988: Global Sea Level change. *Climate variations over the past century and the greenhouse effect: A report based on the first climate trends workshop*, Washington D. C., National Climate Program Office/NOAA, Rockville, Maryland, 7–9.

Boussinesq, J., 1903: *Theorie Aanalyque de la Chaleur. Paris, Gathier-Villars*, **2**, 172. (in French)

Bryan, K., 1996: The steric component of sea level rise associated with enhanced greenhouse warming: A model study. *Climate Dyn.*, **12**, 545–555.

Cazenave, A., and R. S. Nerem, 2004: Present-day sea level change: Observations and causes. *Rev. Geophys.*, **42**, RG3001, doi: 10.1029/2003RG000139.

Cazenave, A., K. DoMinh, S. Guinehut, E. Berthier, W. Llovel, G. Ramillien, M. Ablain, and G. Larnicol, 2009: Sea level budget over 2003–2008: A reevaluation from GRACE space gravimetry, satellite altimetry and ARGO. *Global and Planetary Change*, **65**, 83–88.

Church, J. A., J. S. Godfrey, D. R. Jackett, and T. J. Mcdougall, 1991: A model of sea level rise caused by ocean thermal expansion. *J. Climate*, **4**, 438–456.

Church, J. A., and Coauthors, 2011: Revisiting the earth sea level and energy budgets from 1961 to 2008. *Geophys. Res. Lett.*, **38**, L18601, doi: 10.1029/2011GL048794.

Dobrovolski, S. G., 2000: *Stochastic Climate Theory.* Springer Verlag, Berlin, 282pp.

Fairbridge, R. W., and O. A. Krebs, 1962: Sea Level and the Southern Oscillation. *Geophysical Journal of the Royal Astronomical Society*, **6**, 532–545.

Gill, A. E., 1982: Atmosphere-ocean dynamics. *International Geophysics Series.* Academic Press, 662pp.

Gornitz, V., and S. Lebedeff, 1987: Global sea level changes during the past century. *Sea Level Fluctuation and Coastal Evolution*, D. Nummedal, O. H. Pilkey and J. D. Howard, Eds., Society for Economic Paleontologists and Mineralogists, 3-16 (SEPM Special Publication No. 41).

Gornitz, V., S. Lebedeff, and J. Hansen, 1982: Global sea level trends in the past century. *Science*, **215**, 1611–1614.

Greatbatch, R. J., 1994: A note on the representation of steric sea level in models that conserve volume rather than mass. *J. Geophys. Res.,* **99** (C6), 12767–12771.

Gregory, J. M., and Coauthors, 2001: Comparison of re-

sults from several AOGCMs for global and regional sea-level change 1900–2100. *Climate Dyn.*, **18**, 225–240.

Häkkinen, S., 2001: Variability in sea surface height: A qualitative measure for the meridional overturning in the North Atlantic. *J. Geophys. Res.*, **106**, 13837–13848.

IPCC, 2007: Summary for policymakers. *Climate Change 2007: The Physical Science Basis. Contribution of Working Group I to the Fourth Assessment Report of the Intergovernmental Panel on Climate Change*, S. Solomon, et al., Eds., Cambridge University Press, Cambridge, United Kingdom and New York, NY, USA, 408–417.

Ishii, M., M. Kimoto, K. Sakamoto, and S. I. Iwasaki, 2006: Steric sea level changes estimated from historical ocean subsurface temperature and salinity analyses. *Journal of Oceanography*, **62**(2), 155–170.

Klige, R. K., 1982: Oceanic level fluctuations in the history of the earth. *Sea and Oceanic Level Fluctuations for 15,000 Years*, Acad. Sc. U. S. S. R., Institute of Geography, Moscow, Nauka, 1–22. (in Russian)

Knutti, R., and T. F. Stocker, 2000: Influence of the thermohaline circulation on projected sea level rise. *J. Climate*, **13**, 1997–2001.

Landerer, F. W., J. H. Jungclaus, and J. Marotzke, 2007: Regional dynamic and steric sea level change in response to the IPCC-A1B scenario. *J. Phys. Oceanogr.*, **37**, 296–312.

Levermann, A., A. Griesel, M. Hoffmann, M. Montoya, and S. Rahmstorf, 2005: Dynamic sea level changes following changes in the thermohaline circulation. *Climate Dyn.*, **24**, 347–354.

Li, L. J., and Coauthors, 2013: The Flexible Global Ocean-Atmosphere-Land System Model: Grid-point Version 2: FGOALS-g2. *Adv. Atmos. Sci.*, doi: 10.1007/s00376-012-2140-6.

Li, W,, X. H. Zhang, and X. Z. Jin, 2003: Sea level height on different approximations assumptions in ocean circulation models. *Advances in Marine Science*, **21**(2), 132–141. (in Chinese)

Liu, H. L., Y. Yu, W. Li, and X. Zhang, 2004: *Reference Manual of LASG/IAP Climate System Ocean Model (LICOM1.0). Special technical report of State Key Laboratory of Numerical Modelling for Atmospheric Sciences and Geophysical Fluid Dynamics.* Science Press, Beijing, 107pp. (in Chinese)

Maximenko, N., P. Niiler, M.-H. Rio, O. Melnichenko, L. Centurioni, D. Chambers, V. Zlotnicki, and B. Galperin, 2009: Mean dynamic topography of the ocean derived from satellite and drifting buoy data using three different techniques. *J. Atmos.* Oceanic *Technol.*, **26**(9), 1910–1919.

Mikolajewicz, U., and R. Voss, 2000: The role of the individual air–sea flux components in the CO_2-induced changes of the ocean's circulation and climate. *Climate Dyn.*, **16**, 627–642.

Mikolajewicz, U., B. D. Santer, and E. Maier-Reimer, 1990: Ocean response to greenhouse warming. *Nature*, **345**, 589–593.

Munk, W., 2002: Twentieth century sea level: An enigma. *Proc. Natl. Acad. Sci., USA*, **99**, 6550–6555.

Pattullo, J., W. Munk, R. Revelle, and E. Strong, 1955: The seasonal oscillation in sea level. *J. Mar. Res.*, **14**(1), 88–156.

Taylor, K. E., R. J. Stouffer, and G. A. Meehl, 2012: An overview of CMIP5 and the experiment design. *Ameri. Meteor. Soc.*, 485–498.

Wu, T., J. C. Kang, F. Wang, and Y. M. Zheng, 2006: The new progresses on global sea level change. *Advances in Earth Science*, **21**(7), 730–737.

Yin, J., S. M Griffies, and R. Stouffer, 2010: Spatial variability of sea-level rise in 21st century projections. *J. Climate*, **23**, 4585–4607.